

Physical and Chemical Compatibilization Treatment with Modified Aminosilanes for Aluminum/Polyamide Adhesion

Bo-Young Lee,^{||} Hyun-Gyu Jeong,^{||} Sung Jun Kim,^{||} Beom-Goo Kang, and Keon-Soo Jang*Cite This: *ACS Omega* 2022, 7, 23865–23874

Read Online

ACCESS |



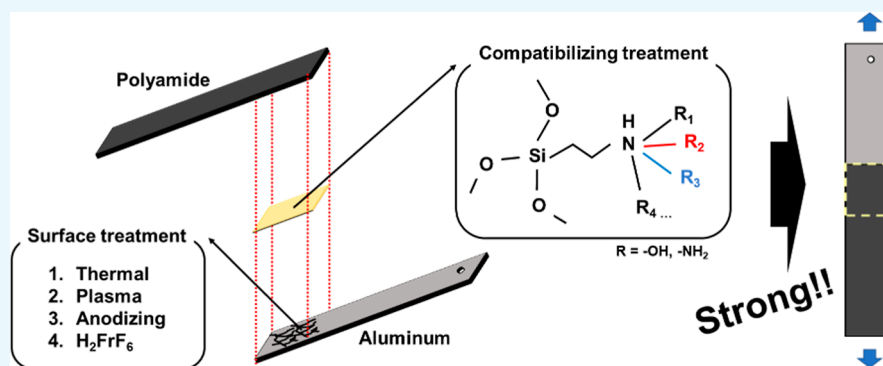
Metrics & More



Article Recommendations



Supporting Information



ABSTRACT: Metal/polymer bilayer composites feature high strength-to-weight ratios and low manufacturing costs despite the weak interfacial adhesion between their components. In this study, aluminum surfaces were modified to generate microporous architectures and hydroxyl moieties by various physical and chemical treatments, including thermal, plasma, anodizing, and hexafluorozirconic acid treatments to overcome the weak interfacial adhesion. The maximum shear strength of the obtained metal/polymer bilayer composites was achieved by anodizing treatment, whereas all treatment methods substantially improved the material toughness. In addition, modified compatibilizing agents with tailorable hydroxyl moieties were applied to enhance the interfacial adhesion using aminoethylaminopropyl trimethoxysilane (AEAPS) and modified AEAPS as a coupling agent. AEAPS modified by monoepoxide (glycidol) produced the strongest positive effect on the composite mechanical properties. These findings can be useful in a myriad of metal/polymer multilayer composites.

1. INTRODUCTION

Aluminum (Al) exhibits a high strength-to-weight ratio, good machining properties, low processing/material costs, and high corrosion resistance as compared with the corresponding parameters of other metals.^{1–4} Thus, it has been extensively exploited most notably in aerospace and automotive applications,^{5–7} which often require the utilization of aluminum/polymer composites due to their significantly lower weights.^{8–10} For instance, aluminum/polymer laminates possess the superior strength-to-weight and modulus-to-weight ratios to various aluminum-infiltrated polymeric composites.^{8,11} In addition, aluminum and polymers can be joined by mechanical fastening and adhesive bonding techniques.¹² Compared with the conventional mechanical fastening methods such as riveting and bolting, adhesive bonding has considerable advantages, including low material weights, aerodynamically smooth surfaces, and good fatigue resistances due to the absence of local stress concentration.^{13,14}

Strong adhesion between polymeric substances and metals is of great importance for various potential applications such as food and pharmaceutical packaging, fire protection, film capacitors, electronic devices, aircraft, and automobiles.^{15–22}

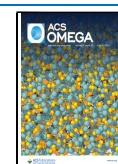
For instance, metal–polymer–metal laminated sheets have been used as vehicle body panels to decrease noise, vibration, and weight.²² In addition, metal–polymer laminate systems with low weight in structural substrates thermally decomposed with generated volatiles when exposed to fire, thereby resulting in delamination and inflation of foils. This mechanism substantially reduced the thermal conductivity.²¹ It can be achieved by tailoring the physical and chemical properties of their interfaces through coupling/compatibilization combined with surface modification.^{23,24}

Polymer surfaces are often subjected to various modifications, such as mechanical treatment, wet chemical treatment, glow discharge plasma treatment, flame exposure, corona discharge treatment, high-temperature oxidation, and organic

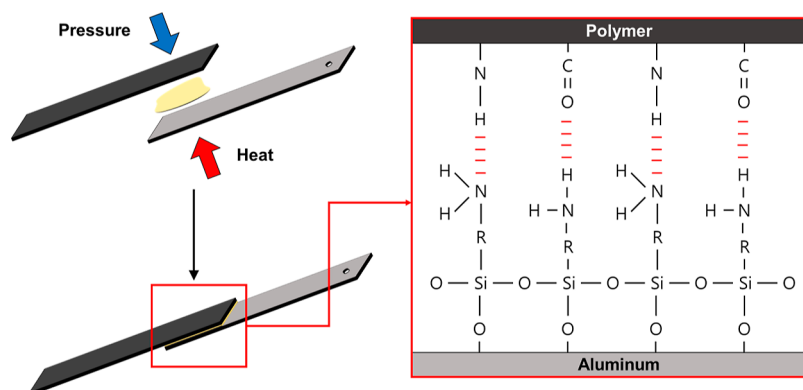
Received: April 25, 2022

Accepted: June 10, 2022

Published: June 29, 2022



Scheme 1. Schematic Describing the Bonding Mechanism of the Prepared PA66/Al Composites



acid etching, to ensure effective mechanical interlocking between aluminum and polymer surfaces.^{25–29} The incorporation of organic coupling agents represents the most facile treatment method. For instance, nonpolar polymers are typically modified by various organic acids, such as acetic, chromic, propionic, citric, and lactic acids,^{30–33} whereas the surfaces of polar polymers are treated with organo-functional silanes containing amino, epoxide (oxyrane), thiol, or sulfonate groups.^{34–36}

Treatments for metal surfaces are primarily performed to obtain microscopically rough oxide surface species, which facilitate the mechanical interlocking at their interfaces.^{37,38} However, a limited number of aluminum surface treatment methods have been reported till date.^{39–42} Unlike other metals, aluminum undergoes anodizing that produces a hard, durable, and corrosion-resistant aluminum oxide layer containing highly ordered columnar porous structures.⁴⁰ The hydration of H₂O converts Al–O to hydrophilic hydrous oxides, such as Al(OH)₃ (bayerite) and AlOOH (boehmite), thereby enhancing the adhesions at the interfaces between polar polymers and aluminum substrates.⁴³ More specifically, the aqueous solutions containing sodium hydroxide (NaOH) or sulfuric-chromic acid (H₂SO₄/CrO₃) effectively corrode aluminum substrates.⁴⁴

In addition to the surface modifications of aluminum and polymers, the coupling (compatibilizing) effects of organic compounds have been utilized for enhancing aluminum–polymer interfaces. Aminopropyl silane and aminopropyl phosphonate are typical organic coupling agents employed for this purpose. However, the previously developed methods involving organic coupling agents include a pre-reaction of these coupling agents with either the polymer or the aluminum surface, thereby significantly limiting their applications. In this study, various aluminum surface treatment techniques, including a chemical modification with zirconium acid and compatibilization with silane-based compounds containing tailorable hydroxyl moieties via one-step lamination were examined.

2. EXPERIMENTAL SECTION

2.1. Materials. Aminoethylaminopropyl trimethoxysilane (AEAPS) was purchased from Dow Corning Co. (100%, OFS-6020, Xiameter, Midland, MI, USA). Deionized water (DI water) and acetic acid (CH₃COOH) were supplied by Duksan Co. (South Korea). Nitric acid (HNO₃, 65%) was purchased from Tokyo Chemical Industry Co., Ltd. (TCI, Japan). Acetone, sodium hydroxide (NaOH), and zirconium acid

(H₂ZrF₆, 20% w/w in DI-water) were purchased from BNOChem Co. (South Korea). Aluminum alloy (Al6061, Al/Mg/Si/Fe/Cu/Cr = ca. 97.2:1.0:0.6:0.35:0.25:0.25 by mass, less than 0.35 wt % Zn/Ti/Mn) sheets with dimensions of 24 mm × 85 mm × 1.96 mm were manufactured by Jun tech Co. (South Korea). Polyamide 6,6 (PA66) was obtained from Lotte Chemical Co. (South Korea). Glycidol (monoepoxide) and 1,4-butyl diglycidyl ether (diepoxide; 1,4-BDGE) were purchased from Sigma-Aldrich (St. Louis, MO, USA) and Kukdo Chemical Co. (South Korea), respectively.

2.2. Surface Modifications of Al Substrates. Four different Al surface treatment methods (heat, plasma, anodizing, and zirconium acid treatments) were used. The treated Al samples were stored in a sealed vacuum package for 3 days prior to AEAPS treatments. All Al specimens were ultrasonicated with acetone for 20 min to remove any organic contaminants prior to surface treatments. The resulting Al sample with cleaned surfaces was labeled “pristine Al sample.”

2.2.1. Thermal Treatment. One group of the pristine Al samples was placed inside an oven and annealed at 150–250 °C for various durations (5–25 min). The thermally treated samples were stored at room temperature for 1–5 days to investigate the effect of ambient conditions on the formation of hydroxyl groups on the Al surface.

2.2.2. Plasma Treatment. Another group of the pristine Al samples was treated with plasma (Compact Plasma Cleaner, PDC-32-G-LD, MTI Co., South Korea). Oxygen (100 mL/min) and argon (100 mL/min) were simultaneously injected and mixed in the chamber (3 in. diameter and 6.5 in. length). The RF power, voltage, and current were adjusted to 18 W, 720 V, and 25 mA, respectively.

2.2.3. Anodizing Treatment. A third group of the pristine Al samples was electrochemically anodized at a voltage of 15 V DC at 70 °C for 10 min to generate hydroxyl groups and grooved surfaces. The electrolyte was composed of an aqueous solution of about 10 wt % (100 g sulfuric acid/1 L H₂O). The anodized samples were rinsed in DI-water for 1 min and dried in an air stream at 22–25 °C.

2.2.4. Zirconium Acid Treatment. The last group of the pristine Al samples was soaked in a 5% w/w NaOH solution at 50 °C for 3 min and then washed and rinsed with DI-water three times. The cleaned Al samples were soaked in 50% v/v HNO₃ at 25 °C for 1 min and then washed with DI-water three times. Finally, these samples were soaked in an H₂ZrF₆/NaOH solution 25 °C for 3 min, which was prepared by mixing 100 mg/L H₂ZrF₆ with 0.1 M NaOH to maintain pH 4.5.

2.3. AEAPS Modifications of Surface-Treated Al Substrates. In addition, 3 mL of AEAPS was mixed with 100 mL of DI-water at pH 3–5 and stirred at 22–25 °C at 200 rpm for 3 min to convert $-\text{Si}(\text{OCH}_3)_3$ moieties to $-\text{Si}(\text{OH})_3$ groups. The solution pH was controlled by acetic acid during this process.

The surfaces of the pristine and treated samples were coated by the prepared AEAPS solution to achieve a film thickness of ca. 7 μm , assuming the rare water-related residues. A drop of AEAPS (minimum loading: 10 mg) was applied on the Al substrate by using a micropipette to avoid flow down. The interfacial area between the PA66 layers and Al substrates was 24 mm \times 25 mm. A weight of 2 kg was applied to the sandwiched samples for 2 min in a temperature range of 100–250 °C (Scheme 1). The silane groups react with the Al surfaces, while the amine moieties interact with the amide groups in PA66 (Scheme 1).

2.4. AEAPS Chemical Modification Procedure. AEAPS was chemically modified by reacting with either glycidol (monoepoxide) or 1,4-BDGE (biepoxide). For this purpose, a 40 wt.% AEAPS solution in DI-water was stirred at 200 rpm at 22–25 °C while maintaining pH 3.0 using acetic acid. Subsequently, glycidol or 1,4-BDGE was mixed with the AEAPS solution at a stoichiometric ratio (1 g/equiv/1 g/equiv) at 22–25 °C for 3 min. The resulting solution was filtered to remove the possibly cross-linked aminosilanes.

2.5. Characterization Techniques. Fourier transform infrared (FTIR, Nicolet 6700, Thermo Fisher Scientific Co., Waltham, MA, USA) spectroscopy studies were performed in the attenuated total reflection (ATR) mode to detect hydroxyl groups. Each FTIR spectrum was recorded in a wavenumber region of 3000–2500 cm^{-1} by conducting 16 scans.

X-ray photoelectron spectroscopy (XPS, K-Alpha Plus, Thermo Fisher Scientific Co., Waltham, MA, USA) measurements were performed at the Center for Advanced Materials Analysis to confirm the composition of the surface hydroxyl groups.

Scanning electron microscopy (SEM, Apreo, FEI Co., Hillsboro, OR, USA) observations were conducted at the Center for Advanced Materials Analysis to examine the morphologies of the analyzed sample surfaces. The samples for SEM studies were sputter-coated with Pt/Pd on the carbon tape to guarantee good conduction.

Atomic force microscopy (AFM; NX10, Park systems Co., South Korea) with the non-contact mode was utilized to examine the surface morphology of Al. The specimen size was 24 mm \times 25 mm \times 2 mm. The scan size and rate were 10 μm \times 10 μm and 0.4 Hz, respectively.

The shear strength and toughness of the bonded samples were measured using a universal testing machine (LR10K Plus, Lloyd Instruments, AMETEK, Inc., Berwyn, PA, USA) at a crosshead rate of 1 mm/min (see Figure S1). The specimen size was 24 mm \times 145 mm \times 4 mm. The toughness values were obtained from the integrated areas of the resulting stress–strain curves.

Contact angles of DI-water drops were determined by a Digi-drop instrument (GBX Surface Science Technology Co., Ireland). Their magnitudes were calculated by performing shape analyses of the sessile drop images obtained at the three-phase contact points between the air, drop contours, and projections of the Al surface.

3. RESULTS AND DISCUSSION

Al surfaces can be mechanically and chemically treated to enhance their compatibility with polymeric materials prior to

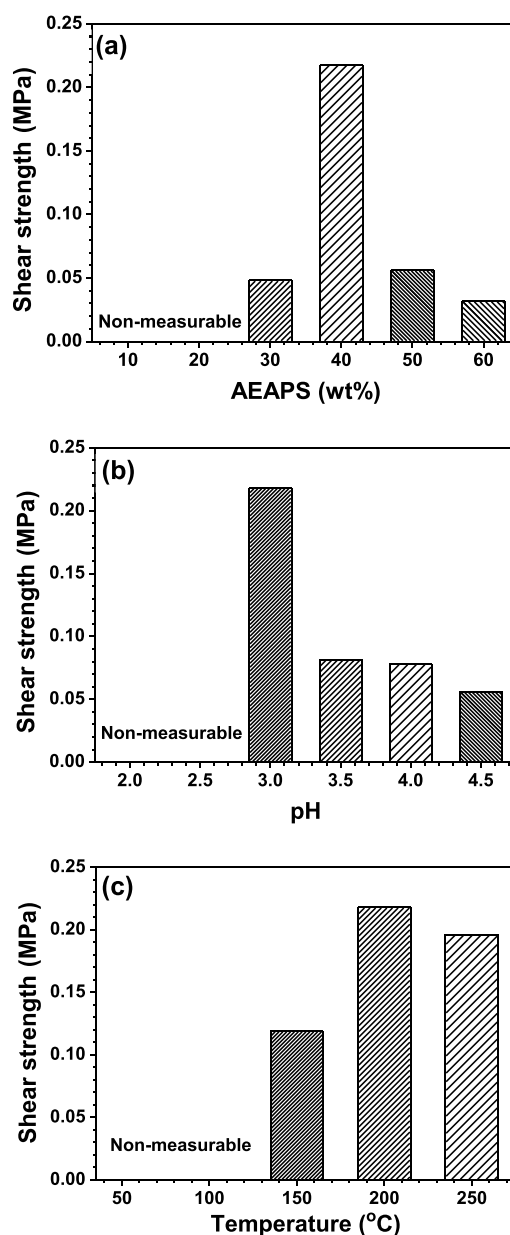


Figure 1. Shear strengths of the metal/polymer composites measured at (a) different AEAPS concentrations, pH 3.0, and 200 °C; (b) different pH values, 40 wt % AEAPS, and 200 °C; and (c) different reaction temperatures, 40 wt % APES, and pH 3.0.

the bonding process. For chemical treatments, the AEAPS compatibilizer (coupling agent) was mixed with acetic acid to produce trialkoxysilanes, which could react with hydroxyl groups on the prepared Al surfaces. The coupling agent (AEAPS) was added between the untreated Al and the PA66 layer. Various factors such as AEAPS concentration, reaction temperature, and pH influenced the shear strengths of composites, as shown in Figure 1. The adhesion between the untreated Al and the polymer was not achieved below the AEAPS concentration of 20 wt %. At an AEAPS concentration of 40 wt %, the shear strength of the composite reached a

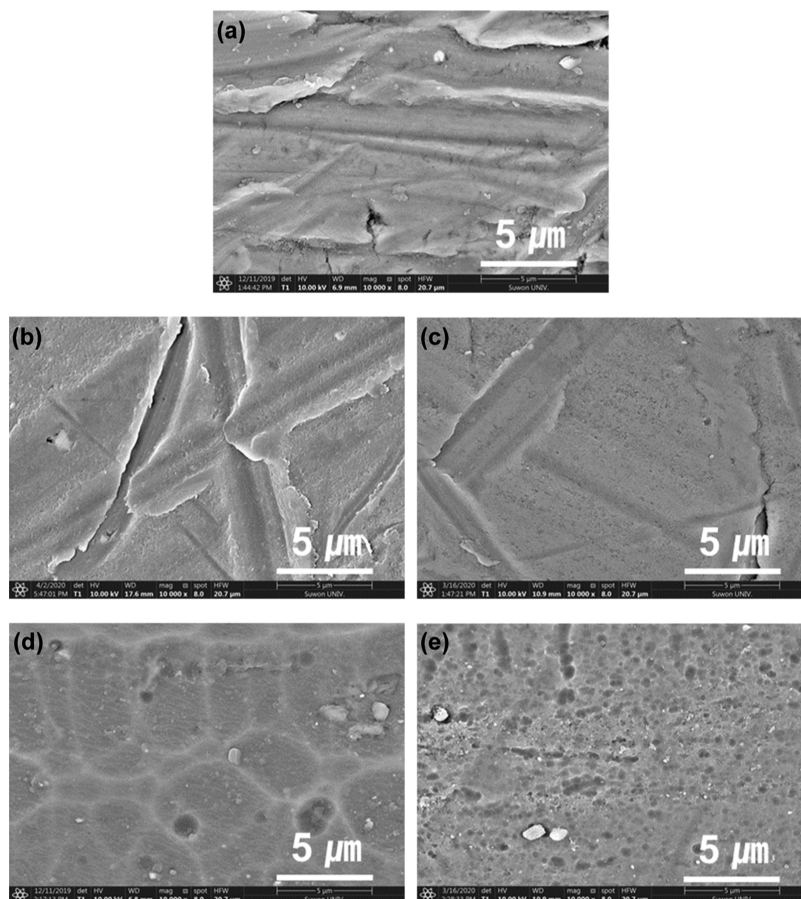


Figure 2. SEM images of Al surfaces by various treatments without AEAPS functionalization: (a) none (neat Al), (b) thermal (200 °C, 15 min), (c) plasma, (d) anodizing, and (e) H_2ZrF_6 .

maximum and then decreased with increasing AEAPS content (Figure 1a). The highest shear strength was obtained at pH 3.0 and temperature of 200 °C. The aminosilane concentration, solution pH, and reaction temperature substantially influenced the reaction mechanism and shear strength.^{45–47} As an example, the coordination between amine groups and silver nanoparticles occurred only at a certain concentration probably due to the complex relationship among the three factors (concentration, pH, and temperature). The optimum conditions required to achieve the highest shear strength in this study corresponded to an AEAPS concentration of 40 wt %, reaction temperature of 200 °C, and a pH value of 3.0.

For further enhancement of the interfacial adhesion, the surface morphologies of the fabricated metal specimens and functional groups on the studied surfaces were examined. The Al surfaces were modified by various methods such as thermal, plasma, anodizing, and hexafluorozirconic acid (H_2ZrF_6) treatments to generate rough surfaces and hydroxyl moieties on the Al surfaces. In particular, the thermal and plasma treatments were performed for the production of hydroxyl groups, whereas the anodizing and H_2ZrF_6 treatments were conducted for the generation of microporous rough surfaces. The surface roughness and morphology were determined by performing SEM and AFM observations (Figures 2–4 and S2, and Table S1). The SEM and AFM images of the Al surfaces obtained after various treatments show that the thermal and plasma treatments rarely influenced the surface micromorphology and roughness, whereas the anodizing and H_2ZrF_6 treatments produced microporous structures on the studied

surfaces and increased their average roughness values. Furthermore, the SEM and AFM images of the Al surfaces subjected to the plasma treatment revealed that their morphologies only slightly changed as a function of plasma treatment time (Figures S3 and S4). The surface treated with plasma for 20 min was smoother than those for 1, 3, 5, and 10 min probably because the bare Al surface was easily subjected to plastic deformation and thus further plasma treatment (>10 min) resulted in reduction in the elevated *z*-position Al (summit), which had been the bare Al surface.

In addition to the production of rough microporous structures, the generation of hydroxyl moieties is another important factor, affecting the compatibility between metals and polymers, which was examined by the FTIR–ATR and XPS techniques. The four different surface treatments were conducted to chemically modify the Al surfaces, as shown in Figure 5. The thermal, plasma, anodizing, and H_2ZrF_6 treatments increased the hydroxyl groups on the Al surfaces. The broad FTIR peaks located near 3000 cm^{-1} are ascribed to hydroxyl groups (Figure 5a). The optimum conditions for thermal treatment corresponded to a temperature of 200 °C and treatment duration of 15 min (Figure S5). Beyond 200 °C and 15 min, the number of hydroxyl groups decreased with further increases in the treatment temperature and time, owing to the likely formation of $-\text{Al}-\text{O}-\text{Al}-$ species from $-\text{Al}-\text{OH}$ groups.⁴⁸ Similarly, the FTIR intensities of the hydroxyl groups on the thermally treated Al surfaces decreased after 3 days of storage because of the formation of $-\text{Al}-\text{O}-\text{Al}-$ groups (Figure S5c). The generated hydroxyl moieties on the treated

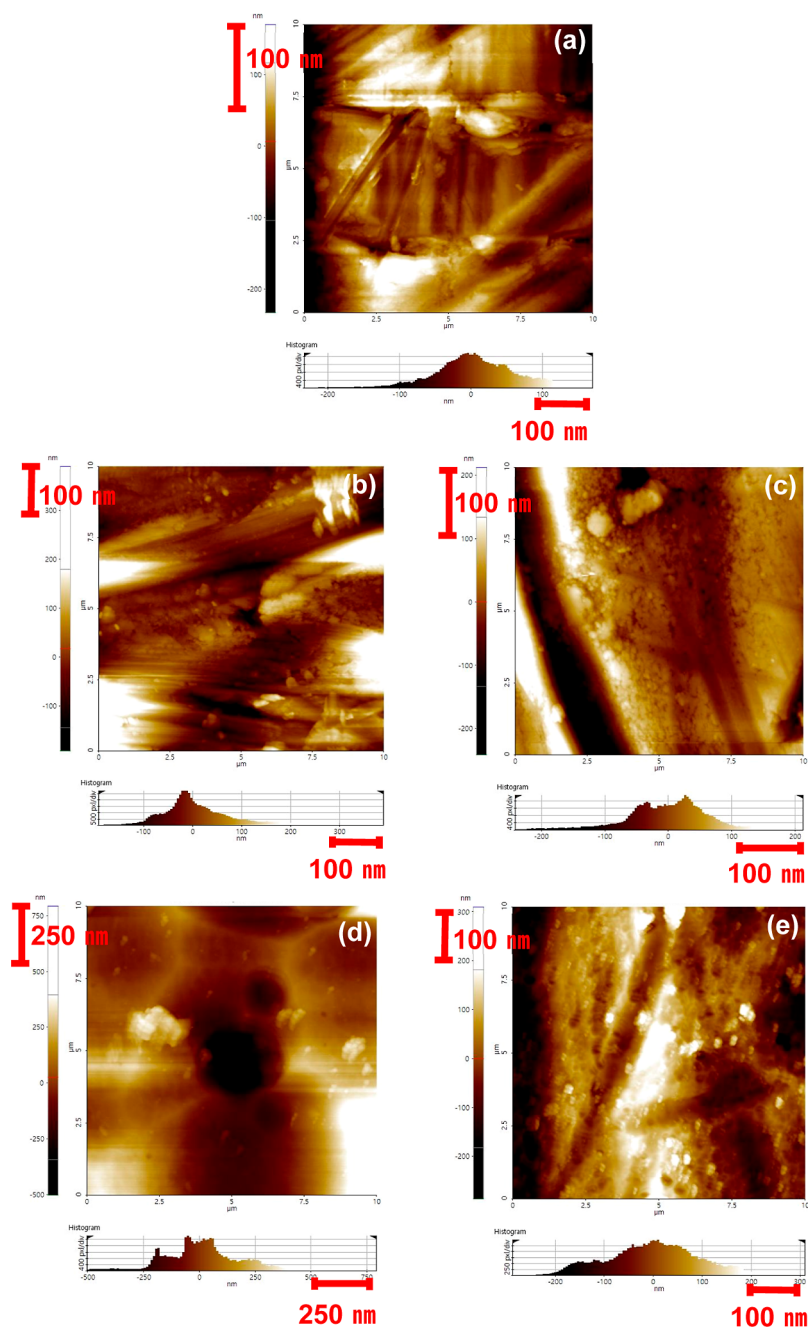


Figure 3. AFM 2D topography images with height profile of Al surfaces by various treatments without AEAPS functionalization: (a) none (neat Al), (b) thermal (200 °C, 15 min), (c) plasma, (d) anodizing, and (e) H_2ZrF_6 .

Al surfaces were confirmed by the XPS profiles, as depicted in Figure S6a–f. The peaks at ca. 533 and 531 eV in deconvoluted spectra (Figure S6b–f) were ascribed to hydroxyl and Al–O groups, respectively.^{49–51} The ratios between hydroxyl moieties and total O-related groups for all samples were quantified, as shown in Figure 5b. Similar to FTIR–ATR results, all treated surfaces had higher –OH concentrations than the pristine Al surface. Among the treated surfaces, the thermally and plasma-treated surfaces showed the highest and lowest –OH concentrations, respectively.

The synergistic effects of the physical and chemical treatments were investigated by measuring contact angles, as shown in Figure 6. The Al surface subjected to the anodizing treatment exhibited the lowest contact angle, indicating its

excellent wettability properties due to the combination of the physical and chemical treatments. Although the thermal and plasma treatments contributed only to the chemical modifications of the studied surfaces, the effect of hydroxyl groups produced by the 5 min plasma treatment substantially decreased the contact angle, as shown in Figure S7. However, the thermal treatment weakly influenced the water contact angle despite the generated hydroxyl groups on the corresponding Al surface. To investigate the effect of storage time on the contact angle, the surface-treated samples were stored under ambient conditions. The additional storage time (5 days) reduced the concentration of hydroxyl groups, as shown in Figure S8. The wettability was enhanced by high-surface energy (hydrophilic) of the Al substrate, which was

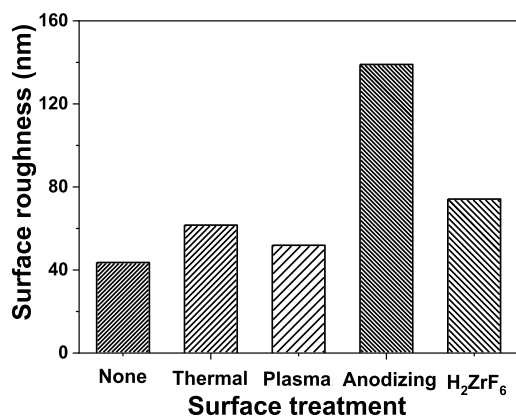


Figure 4. Average surface roughness of Al surfaces subjected to various treatments without AEAPS functionalization: none (neat Al), thermal (200 °C, 15 min), plasma, anodizing, and H₂ZrF₆.

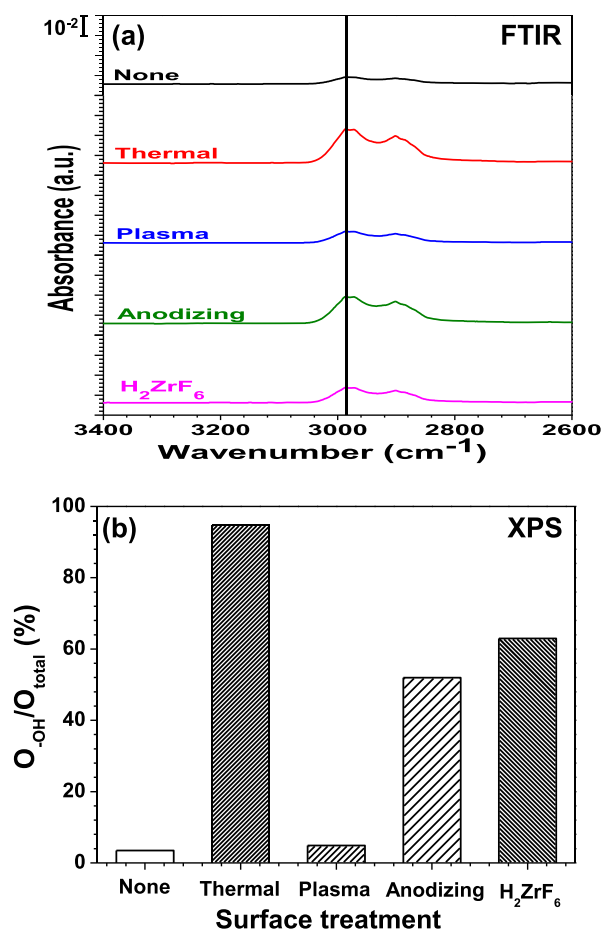


Figure 5. FTIR-ATR spectra (a) and XPS profiles (b) of Al surfaces subjected to various treatments without AEAPS functionalization: none (neat Al), thermal (200 °C, 15 min), plasma, anodizing, and H₂ZrF₆ treatments. O_{-OH}/O_{total}: 100% × integrated area at ca. 533 eV ÷ integrated areas at ca. 533 and 531 eV.

caused by the surface treatments. Strong secondary interactions such as hydrogen bonding improved the wettability, thereby reducing the water contact angle.^{52,53} Based on the FTIR and contact angle results, it was concluded that the competition between the generations of hydroxyl groups and metal oxide species on the thermally treated Al surfaces determined the contact angle value.

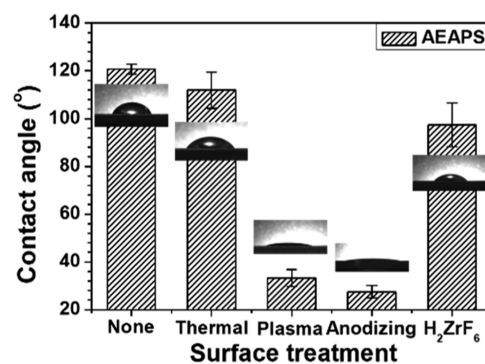


Figure 6. Water contact angles of Al surfaces by various treatments: none (neat Al), thermal (200 °C, 15 min), plasma, anodizing, and H₂ZrF₆ with AEAPS functionalization.

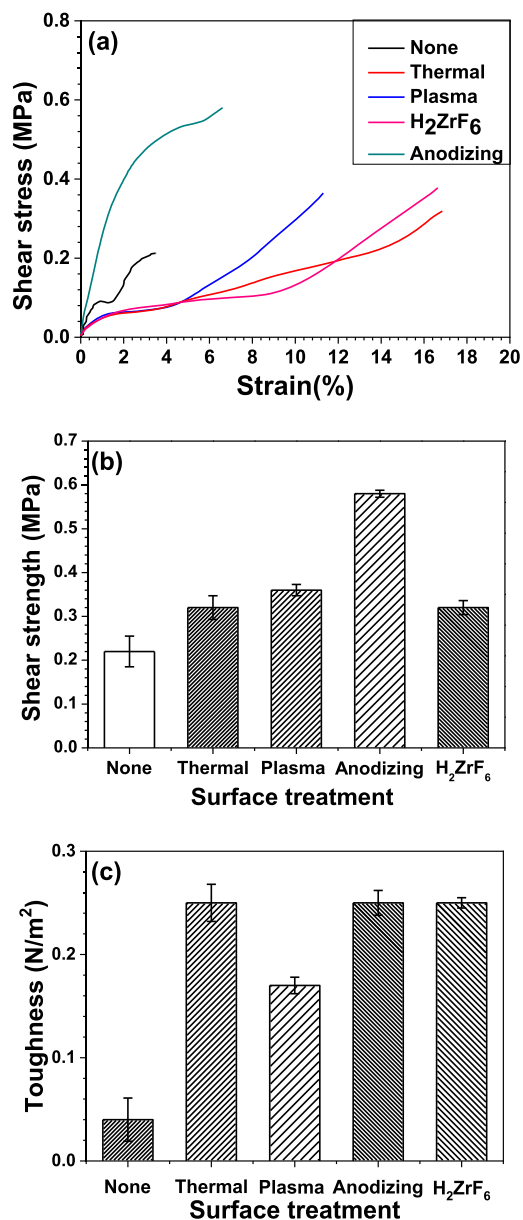
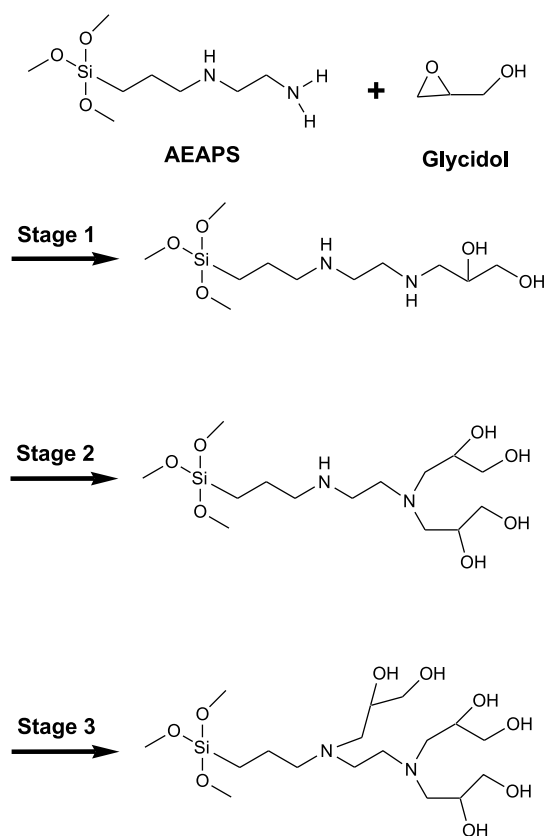


Figure 7. Shear stress-strain curve (a), shear strength (b), and toughness (c) of Al surfaces by various treatments with AEAPS functionalization: none (neat Al), thermal (200 °C, 15 min), plasma (10 min), anodizing, and H₂ZrF₆.

Scheme 2. Reaction Mechanism of AEAPS with Glycidol: AEAPS-G



Scheme 3. Reaction Mechanism of AEAPS with 1,4-BDGE: AEAPS-B

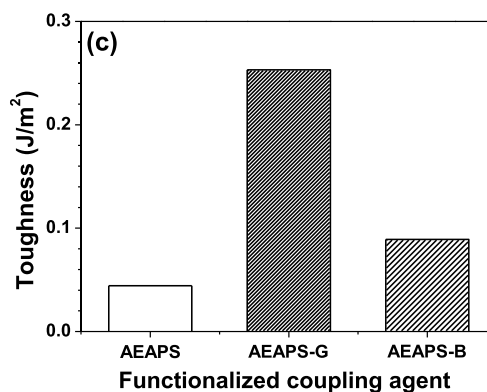
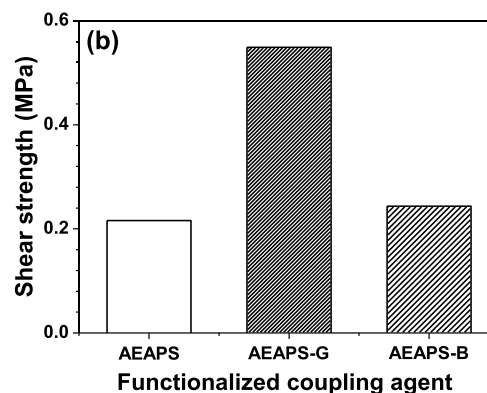
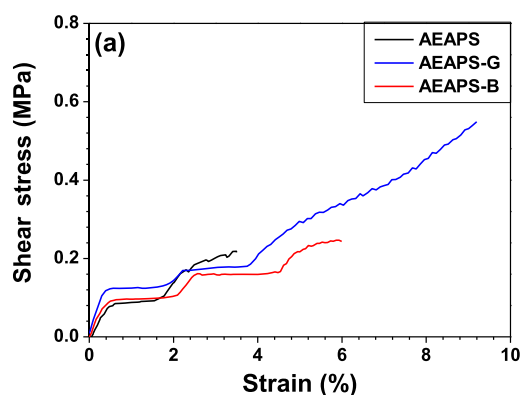
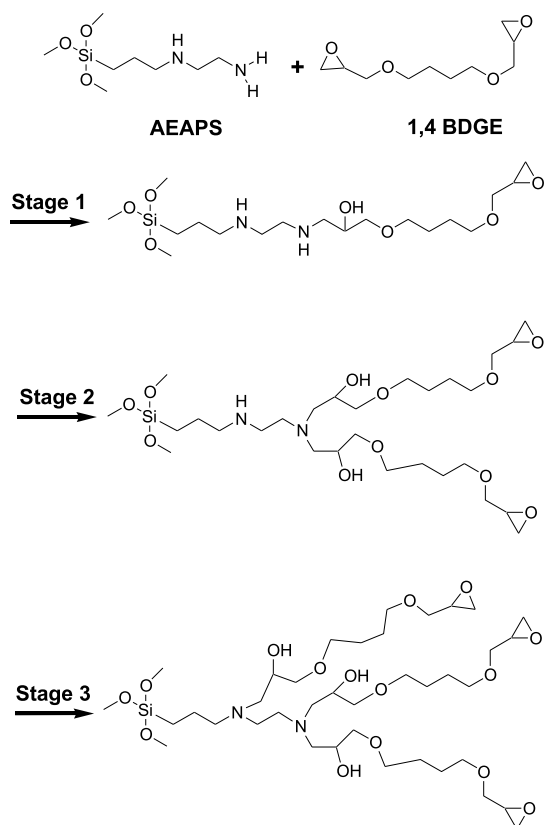


Figure 8. Shear stress–strain curve (a), shear strength (b), and toughness calculated based on the shear stress–strain curve (c) of Al/PA66 composites with different functionalized coupling agents.

The compatibilizing agent (namely, coupling agent) can enhance the interfacial interactions between metals and polymers. The mechanical properties of metal/polymer composites fabricated by using AEAPS (compatibilizing agent) are examined in Figure 7. On the basis of the shear stress–strain curve (Figure 7a), the shear strength and toughness values of these materials were calculated. In terms of shear strength, the anodizing treatment was the most effective, whereas the toughness of the composites treated with four different methods was similar to each other. The surface treatments for Al enhanced the shear strength and toughness. The 10 min plasma treatment showed the highest mechanical properties as compared with those obtained at other plasma treatment times, as shown in Figure S9.

Finally, AEAPS was chemically modified by monoepoxide (glydiol) and bi-epoxide (1,4-BDGE) to further improve the interfacial interaction between the Al and PA66 components.

The reaction mechanisms established for the AEAPS/glycidol (AEAPS-G) and AEAPS/1,4-BDGE (AEAPS-B) systems are displayed in Schemes 2 and 3, respectively. As the reactions progress, the organic-like part becomes more hydrophilic, thereby improving the interfacial interaction between the compatibilizing agent and PA66. The shear strength and toughness of AEAPS-G substantially increased, whereas those of AEAPS-B only slightly increased (Figure 8). This is because of the higher concentration of hydroxyl moieties generated on the AEAPS-G surface. In addition, 1,4-BDGE might react with two different AEAPS molecules, thereby weakening the compatibilizing effect. Thus, the monoepoxide modification of AEAPS was more effective than the bi-epoxide modification in terms of achieving a stronger coupling effect.

4. CONCLUSIONS

The chemical and physical treatments resulted in microporous structures and high concentrations of hydroxyl moieties on the studied Al surfaces. The thermal, plasma, anodizing, and H₂ZrF₆ treatments increased the material toughness, whereas the shear strength of metal/polymer bilayer composites was considerably enhanced by the anodizing treatment. The microporous structures were observed by SEM and AFM images. The generation of hydroxyl groups was monitored by FTIR and XPS spectra. The treated samples showed rough surfaces and more hydroxyl moieties. The synergic effects of physical and chemical treatments were investigated by contact angle measurements and mechanical properties. The treated samples showed lower contact angles and better mechanical properties. Furthermore, the utilized compatibilizing agents were chemically modified through the reactions of AEAPS with monoepoxide and bi-epoxide compounds to increase the numbers of hydroxyl moieties and promote the interfacial adhesion of the Al/PA66 bilayer composites. It was found that the AEAPS-G species generated by the reactions between AEAPS and glycidol (monoepoxide) substantially enhanced the mechanical properties of the composites. The finding in this study may be applied to the injection molding for metal/polymer bilayer composites.

■ ASSOCIATED CONTENT

SI Supporting Information

The Supporting Information is available free of charge at <https://pubs.acs.org/doi/10.1021/acsomega.2c02567>.

Shear test of metal/polymer composites; AFM topography 3D images with height profile of Al surfaces by various treatments without AEAPS functionalization: none (neat Al), thermal (200 °C, 15 min), plasma, anodizing, and H₂ZrF₆; SEM images of Al surfaces by plasma treatment: pristine Al and 1, 3, 5, 10, and 20 min; AFM images of Al surfaces treated with plasma: pristine Al, 5 min, 10 min, and 20 min; FTIR results: various temperatures for 15 min, various times at 200 °C, and ambient storage times of the sample surface treated at 200 °C for 15 min; XPS profiles of Al surfaces with various treatments without AEAPS functionalization: full spectra for all samples, none (neat Al), thermal 200 °C, 15 min), plasma, anodizing, and H₂ZrF₆ treatments; contact angle of Al surfaces treated with plasma with different times; contact angle of samples surface treated at 200 °C for 15 min with various storage times; shear stress–strain curve of Al/PA66 composites with differ-

ent plasma treatment times for Al; and Ra values based on AFM software (PDF)

■ AUTHOR INFORMATION

Corresponding Author

Keon-Soo Jang – Department of Polymer Engineering, School of Chemical and Materials Engineering, The University of Suwon, Hwaseong-si 18323, Republic of Korea; orcid.org/0000-0002-0883-2683; Email: ksjang@suwon.ac.kr, ksjang4444@gmail.com

Authors

Bo-Young Lee – Department of Polymer Engineering, School of Chemical and Materials Engineering, The University of Suwon, Hwaseong-si 18323, Republic of Korea; Present Address: R&D Center, SEMCNS Co., Ltd., Suwon-si, Gyeonggi-do, 16674, Republic of Korea

Hyun-Gyu Jeong – Department of Polymer Engineering, School of Chemical and Materials Engineering, The University of Suwon, Hwaseong-si 18323, Republic of Korea

Sung Jun Kim – Mobility Marketing Team, Samyang Co., Seoul 03129, Republic of Korea

Beom-Goo Kang – Department of Chemical Engineering, Soongsil University, Seoul 06978, Republic of Korea; orcid.org/0000-0001-5482-3019

Complete contact information is available at:

<https://pubs.acs.org/10.1021/acsomega.2c02567>

Author Contributions

[†]B.-Y.L., H.-G.J., and S.J.K. contributed equally.

Notes

The authors declare no competing financial interest.

■ ACKNOWLEDGMENTS

This work was supported by the Technology Innovation Program (or Industrial Strategic Technology Development Program-Material Components Technology Development Program) (no. 20011433, Extremely cold-resistant anti-vibration elastomer with EPDM) funded by the Ministry of Trade, Industry & Energy (MOTIE, Korea). This work was supported by the National Research Foundation of Korea (NRF) grant funded by the Korea government (MSIT) (no. 2021R1G1A1011525, Rapid low-temperature curing of thermoset resins via microwave). This work was supported by the Technology Innovation Program (or Industrial Strategic Technology Development Program- Nano fusion innovative product technology development) (no. 20014475, Anti-fog nano-composite-based head lamp with <10% of low moisture adsorption in surface area) funded by the Ministry of Trade, Industry & Energy (MOTIE, Korea). This work was supported by the Technology Innovation Program (or Industrial Strategic Technology Development Program- Automobile industry technology development) (20015803, High performance composite-based battery pack case for electric vehicles via hybrid structure and weight lightening technology) funded by the Ministry of Trade, Industry & Energy (MOTIE, Korea). This work was supported by the Technology development Program (Antistatic extrudable carbon nanotube/polymer composites with 10⁶–10⁸ Ω/sq of surface resistance for display tray: S3111196) funded by the Ministry of SMEs and Startups (MSS, Korea). This work was supported by the INNOPOLIS Foundation grant funded by the Korea govern-

ment (MSIT) (Development of sintered Cu bonding material with Pb-free for power semiconductor module: 2021-DD-RD-0385-01). This research was supported by Research and Business Development Program through the Korea Institute for Advancement of Technology (KIAT) funded by the Ministry of Trade, Industry and Energy (MOTIE) (Development of one step black epoxy bonding film for micro LED display, grant number: P0018198). This work was supported by the Technological Innovation R&D Program (Development of metal-polymer heterojunction bonding technology using metal surface treatment and compatibilizing agents for lightweighting: S3236143) funded by the Ministry of SMEs and Startups (MSS, Korea). This work was supported by Advanced Materials Analysis Center, University of Suwon.

REFERENCES

- (1) Elangovan, K.; Balasubramanian, V.; Babu, S. Developing an Empirical Relationship to Predict Tensile Strength of Friction Stir Welded AA2219 Aluminum Alloy. *J. Mater. Eng. Perform.* **2008**, *17*, 820–830.
- (2) Kishawy, H. A.; Dumitrescu, M.; Ng, E.-G.; Elbestawi, M. A. Effect of Coolant Strategy on Tool Performance, Chip Morphology and Surface Quality during High-Speed Machining of A356 Aluminum Alloy. *Int. J. Mach. Tool Manufact.* **2005**, *45*, 219–227.
- (3) Ghali, E. *Corrosion Resistance of Aluminum and Magnesium Alloys: Understanding, Performance, and Testing*; John Wiley & Sons, 2010.
- (4) Bouchama, L.; Azzouz, N.; Boukmouche, N.; Chopart, J. P.; Daltin, A. L.; Bouznit, Y. Enhancing Aluminum Corrosion Resistance by Two-Step Anodizing Process. *Surf. Coat. Technol.* **2013**, *235*, 676–684.
- (5) Wang, G.; Zhao, Y.; Hao, Y. Friction Stir Welding of High-Strength Aerospace Aluminum Alloy and Application in Rocket Tank Manufacturing. *J. Mater. Sci. Technol.* **2018**, *34*, 73–91.
- (6) Shin, J.; Kim, T.; Kim, D.; Kim, D.; Kim, K. Castability and Mechanical Properties of New 7xxx Aluminum Alloys for Automotive Chassis/Body Applications. *J. Alloys Compd.* **2017**, *698*, 577–590.
- (7) Long, R. S.; Boettcher, E.; Crawford, D. Current and Future Uses of Aluminum in the Automotive Industry. *JOM* **2017**, *69*, 2635–2639.
- (8) Karami Pabandi, H.; Movahedi, M.; Kokabi, A. H. A New Refill Friction Spot Welding Process for Aluminum/Polymer Composite Hybrid Structures. *Compos. Struct.* **2017**, *174*, 59–69.
- (9) Zeng, F.; Chen, J.; Yang, F.; Kang, J.; Cao, Y.; Xiang, M. Effects of Polypropylene Orientation on Mechanical and Heat Seal Properties of Polymer-Aluminum-Polymer Composite Films for Pouch Lithium-Ion Batteries. *Materials* **2018**, *11*, 144.
- (10) Huang, X.; Rao, W.; Chen, Y.; Ding, W.; Zhu, H.; Yu, M.; Chen, J.; Zhang, Q. Infrared Emitting Properties and Environmental Stability Performance of Aluminum/Polymer Composite Coating. *J. Mater. Sci. Mater. Electron.* **2016**, *27*, 5543–5548.
- (11) Goushegir, S. M. Friction Spot Joining (FSJ) of Aluminum-CFRP Hybrid Structures. *Weld. World* **2016**, *60*, 1073–1093.
- (12) Jiang, B.; Chen, Q.; Yang, J. Advances in Joining Technology of Carbon Fiber-Reinforced Thermoplastic Composite Materials and Aluminum Alloys. *Int. J. Adv. Manuf. Technol.* **2020**, *110*, 2631–2649.
- (13) Wan, H.; Lin, J.; Min, J. Effect of Laser Ablation Treatment on Corrosion Resistance of Adhesive-Bonded Al Alloy Joints. *Surf. Coat. Technol.* **2018**, *345*, 13–21.
- (14) Martínez-Landeros, V. H.; Vargas-Islas, S. Y.; Cruz-González, C. E.; Barrera, S.; Mourtazov, K.; Ramírez-Bon, R. Studies on the Influence of Surface Treatment Type, in the Effectiveness of Structural Adhesive Bonding, for Carbon Fiber Reinforced Composites. *J. Manuf. Process* **2019**, *39*, 160–166.
- (15) Qiu, S.; Zhou, Y.; Waterhouse, G. I. N.; Gong, R.; Xie, J.; Zhang, K.; Xu, J. Optimizing Interfacial Adhesion in PBAT/PLA Nanocomposite for Biodegradable Packaging Films. *Food Chem.* **2021**, *334*, 127487.
- (16) Albéndiz García, A.; Rodríguez-Castellón, E.; Peláez Millas, D. Surface Modification of Thermoplastics by Low-Pressure Microwave O₂ Plasma Treatment for Enhancement of the Adhesion of the Interface Box/Encapsulating Resin and the Influence on Film Capacitors Operating under Extreme Humidity Conditions. *Appl. Surf. Sci.* **2020**, *513*, 145764.
- (17) Nieminen, J.; Anugwom, I.; Kallioinen, M.; Mänttari, M. Green Solvents in Recovery of Aluminium and Plastic from Waste Pharmaceutical Blister Packaging. *Waste Manag.* **2020**, *107*, 20–27.
- (18) Jang, K.-S.; Eom, Y.-S.; Choi, K.-S.; Bae, H.-C. Synchronous Curable Deoxidizing Capability of Epoxy-Anhydride Adhesive: Deoxidation Quantification via Spectroscopic Analysis. *J. Appl. Polym. Sci.* **2018**, *135*, 46639.
- (19) Jang, K.-S.; Eom, Y.-S.; Choi, K.-S.; Bae, H.-C. Crosslinkable Deoxidizing Hybrid Adhesive of Epoxy-Diacid for Electrical Interconnections in Semiconductor Packaging. *Polym. Int.* **2018**, *67*, 1241–1247.
- (20) Jang, K.-S.; Eom, Y.-S.; Choi, K.-S.; Bae, H.-C. Versatile Epoxy/Phenoxy/Anhydride-Based Hybrid Adhesive Films for Deoxidation and Electrical Interconnection. *Ind. Eng. Chem. Res.* **2018**, *57*, 7181–7187.
- (21) Christke, S.; Gibson, A. G.; Grigoriou, K.; Mouritz, A. P. Multi-Layer Polymer Metal Laminates for the Fire Protection of Lightweight Structures. *Mater. Des.* **2016**, *97*, 349–356.
- (22) Ruokolainen, R. B.; Sigler, D. R. The Effect of Adhesion and Tensile Properties on the Formability of Laminated Steels. *J. Mater. Eng. Perform.* **2008**, *17*, 330–339.
- (23) Zhang, M. C.; Kang, E. T.; Neoh, K. G.; Tan, K. L. Surface Modification of Aluminum Foil and PTFE Film by Graft Polymerization for Adhesion Enhancement. *Colloids Surf., A* **2001**, *176*, 139–150.
- (24) Liu, W.; Luo, Y.; Sun, L.; Wu, R.; Jiang, H.; Liu, Y. Fabrication of the Superhydrophobic Surface on Aluminum Alloy by Anodizing and Polymeric Coating. *Appl. Surf. Sci.* **2013**, *264*, 872–878.
- (25) Siau, S.; Vervaeet, A.; Calster, A. V.; Swennen, I.; Schacht, E. Influence of Wet Chemical Treatments on the Evolution of Epoxy Polymer Layer Surface Roughness for Use as a Build-up Layer. *Appl. Surf. Sci.* **2004**, *237*, 457–462.
- (26) Navaneetha Pandiyaraj, K.; Selvarajan, V.; Deshmukh, R. R.; Gao, C. Adhesive Properties of Polypropylene (PP) and Polyethylene Terephthalate (PET) Film Surfaces Treated by DC Glow Discharge Plasma. *Vacuum* **2008**, *83*, 332–339.
- (27) Park, S.-J.; Jin, J.-S. Effect of Corona Discharge Treatment on the Dyeability of Low-Density Polyethylene Film. *J. Colloid Interface Sci.* **2001**, *236*, 155–160.
- (28) Pehrsson, P. E.; Henderson, L. J.; Keller, T. M. High-Temperature Oxidation of Carborane-Siloxane-Acetylene-Based Polymer. *Surf. Interface Anal.* **1996**, *24*, 145–151.
- (29) Mijovic, J. S.; Koutsky, J. A. Etching of Polymeric Surfaces: A Review. *Polym.-Plast. Technol. Eng.* **1977**, *9*, 139–179.
- (30) Olafsson, G.; Jägerstad, M.; Öste, R.; Wesslen, B.; Hjertberg, T. Effects of Different Organic Acids on the Adhesion between Polyethylene Film and Aluminium Foil. *Food Chem.* **1993**, *47*, 227–233.
- (31) Olafsson, G.; Jägerstad, M.; Öste, R.; WESSLÉN, B. Delamination of Polyethylene and Aluminum Foil Layers of Laminated Packaging Material by Acetic Acid. *J. Food Sci.* **1993**, *58*, 215–219.
- (32) Olafsson, G.; Hildingsson, I. Sorption of Fatty Acids into Low Density Polyethylene and Its Effect on Adhesion with Aluminum Foil in Laminated Packaging Material. *J. Agric. Food Chem.* **1995**, *43*, 306.
- (33) Hjertberg, T.; Lakso, J.-E. Functional Group Efficiency in Adhesion between Polyethylene and Aluminum. *J. Appl. Polym. Sci.* **1989**, *37*, 1287–1297.
- (34) Arnott, D. R.; Ryan, N. E.; Hinton, B. R. W.; Sexton, B. A.; Hughes, A. E. Auger and XPS Studies of Cerium Corrosion Inhibition on 7075 Aluminum Alloy. *Appl. Surf. Sci.* **1985**, *22–23*, 236–251.

- (35) Danilidis, I.; Sykes, J. M.; Hunter, J. A.; Scamans, G. M. Manganese Based Conversion Treatment. *Surf. Eng.* **1999**, *15*, 401–405.
- (36) Mohseni, M.; Mirabedini, M.; Hashemi, M.; Thompson, G. E. Adhesion Performance of an Epoxy Clear Coat on Aluminum Alloy in the Presence of Vinyl and Amino-Silane Primers. *Prog. Org. Coat.* **2006**, *57*, 307–313.
- (37) Dillingham, R. G.; Boerio, F. J. Interphase Composition in Aluminum/Epoxy Adhesive Joints. *J. Adhes.* **1987**, *24*, 315–335.
- (38) Kim, W.-S.; Kim, K.-H.; Jang, C.-J.; Jung, H.-T.; Lee, J.-J. Micro- and Nano-Morphological Modification of Aluminum Surface for Adhesive Bonding to Polymeric Composites. *J. Adhes. Sci. Technol.* **2013**, *27*, 1625–1640.
- (39) Thompson, G. E.; Furneaux, R. C.; Wood, G. C.; Richardson, J. A.; Goode, J. S. Nucleation and Growth of Porous Anodic Films on Aluminium. *Nature* **1978**, *272*, 433–435.
- (40) Keller, F.; Hunter, M. S.; Robinson, D. L. Structural Features of Oxide Coatings on Aluminum. *J. Electrochem. Soc.* **1953**, *100*, 411.
- (41) Venables, J. D.; McNamara, D. K.; Chen, J. M.; Sun, T. S.; Hopping, R. L. Oxide Morphologies on Aluminum Prepared for Adhesive Bonding. *Appl. Surf. Sci.* **1979**, *3*, 88–98.
- (42) Gent, A. N.; Lin, C.-W. Model Studies of the Effect of Surface Roughness and Mechanical Interlocking on Adhesion. *J. Adhes.* **1990**, *32*, 113–125.
- (43) Hennemann, O.-D.; Brockmann, W. Surface Morphology and Its Influence on Adhesion. *J. Adhes.* **1981**, *12*, 297–315.
- (44) Wei, R.; Wang, X.; Chen, C.; Zhang, X.; Xu, X.; Du, S. Effect of Surface Treatment on the Interfacial Adhesion Performance of Aluminum Foil/CFRP Laminates for Cryogenic Propellant Tanks. *Mater. Des.* **2017**, *116*, 188–198.
- (45) Frattini, A.; Pellegrini, N.; Nicastro, D.; Sanctis, O. d. Effect of Amine Groups in the Synthesis of Ag Nanoparticles Using Aminosilanes. *Mater. Chem. Phys.* **2005**, *94*, 148–152.
- (46) Kwon, O. M.; See, S. J.; Kim, S. S.; Hwang, H. Y. Effects of Surface Treatment with Coupling Agents of PVDF-HFP Fibers on the Improvement of the Adhesion Characteristics on PDMS. *Appl. Surf. Sci.* **2014**, *321*, 378–386.
- (47) Naviroj, S.; Koenig, J. L.; Ishida, H. Molecular Structure of an Aminosilane Coupling Agent as Influenced by Carbon Dioxide in Air, PH, and Drying Conditions. *J. Macromol. Sci., Part B: Phys.* **1983**, *22*, 291–304.
- (48) Nylund, A.; Olefjord, I. Surface Analysis of Oxidized Aluminium. 1. Hydration of Al₂O₃ and Decomposition of Al(OH)₃ in a Vacuum as Studied by ESCA. *Surf. Interface Anal.* **1994**, *21*, 283–289.
- (49) Batra, N.; Gope, J.; Vandana; Panigrahi, J.; Singh, R.; Singh, P. K. Influence of Deposition Temperature of Thermal ALD Deposited Al₂O₃ Films on Silicon Surface Passivation. *AIP Adv.* **2015**, *5*, 067113.
- (50) Raja, J.; Nguyen, C. P. T.; Lee, C.; Balaji, N.; Chatterjee, S.; Jang, K.; Kim, H.; Yi, J. Improved Data Retention of InSnZnO Nonvolatile Memory by H₂O₂ Treated Al₂O₃ Tunneling Layer: A Cost-Effective Method. *IEEE Electron Device Lett.* **2016**, *37*, 1272–1275.
- (51) Peng, J.; Sun, Q.; Zhai, Z.; Yuan, J.; Huang, X.; Jin, Z.; Li, K.; Wang, S.; Wang, H.; Ma, W. Low Temperature, Solution-Processed Alumina for Organic Solar Cells. *Nanotechnology* **2013**, *24*, 484010.
- (52) Chen, C.; Zhang, N.; Li, W.; Song, Y. Water Contact Angle Dependence with Hydroxyl Functional Groups on Silica Surfaces under CO₂ Sequestration Conditions. *Environ. Sci. Technol.* **2015**, *49*, 14680–14687.
- (53) Nakamura, S.; Tsuji, Y.; Yoshizawa, K. Role of Hydrogen-Bonding and OH- π Interactions in the Adhesion of Epoxy Resin on Hydrophilic Surfaces. *ACS Omega* **2020**, *5*, 26211–26219.